

**1    Supplementary materials for:**

**2    Pharmacokinetic Properties of  $^{68}\text{Ga}$ -labelled Folic  
3    Acid Conjugates: Improvement Using HEHE  
4    Purification Tag**

**5    Anton Larenkov, Marat Rakhimov, Kristina Lunyoa, Olga Klementyeva, Alesya Maruk, Aleksei  
6    Machulkin**

**7    Content:**

<b>NMR</b>	Experiment details.....	2
<b>Figure S1.</b>	$^1\text{H}$ NMR spectrum (400 MHz) of <b>1</b> in DMSO-d6.....	2
<b>Figure S2.</b>	$^{13}\text{C}$ NMR spectrum (101 MHz) of <b>1</b> in CDCl <sub>3</sub> .....	2
<b>Figure S3.</b>	$^1\text{H}$ NMR spectrum (400 MHz) of <b>1</b> in DMSO-d6/D <sub>2</sub> O.....	3
<b>Figure S4.</b>	$^1\text{H}$ NMR spectrum (400 MHz) of <b>7</b> in DMSO-d6.....	3
<b>HRMS (ESI)</b>	Experiment details.....	4
<b>Figure S5.</b>	HRMS (ESI) spectrum of <b>1</b> .....	4
<b>Figure S6.</b>	HRMS (ESI) spectrum of <b>2</b> .....	4
<b>Figure S7.</b>	HRMS (ESI) spectrum of <b>3</b> .....	5
<b>Figure S8.</b>	HRMS (ESI) spectrum of <b>4</b> .....	5
<b>Figure S9.</b>	HRMS (ESI) spectrum of <b>7</b> .....	6
<b>Figure S10.</b>	HRMS (ESI) spectrum of <b>8</b> .....	6
<b>Figure S11.</b>	HRMS (ESI) spectrum of <b>9</b> .....	7
<b>HPLC-MS</b>	Experiment details.....	8
<b>Figure S12.</b>	LC-MS chromatogram of <b>4 (FA-I)</b> .....	8
<b>Figure S13.</b>	LC-MS chromatogram of <b>9 (FA-II)</b> .....	9
<b>Radio-TLC</b>		
<b>Table S1.</b>	Radio-TLC chromatograms of $[^{68}\text{Ga}]$ Ga-FA-I and $[^{68}\text{Ga}]$ Ga-FA-II.....	10
<b>Table S2.</b>	Examples of radio-TLC chromatograms pre- and post-reformulation.....	11
<b>Radio-HPLC</b>		
<b>Figure S14.</b>	HPLC chromatograms obtained with Method 1 for $[^{68}\text{Ga}]$ Ga-FA-I and $[^{68}\text{Ga}]$ Ga-FA-II, and with Method 2 for $[^{68}\text{Ga}]$ Ga-FA-I and $[^{68}\text{Ga}]$ Ga-FA-II.....	12
<b>Figure S15.</b>	HPLC chromatograms obtained with Method 1 for $[^{68}\text{Ga}]$ Ga-FA-I and $[^{68}\text{Ga}]$ Ga-FA-II pre- and post-reformulation.....	12
<b>The case of <math>[^{68}\text{Ga}]</math>Ga-FA-I accumulation in non-tumor neoplasm (cyst)</b>	.....	13
<b>Table S3.</b>	Biodistribution of $[^{68}\text{Ga}]$ Ga-FA-I in KB-tumor bearing BALB/c nude mouse with spontaneous neoplasm 30 min after injection.....	13
<b>Figure S16.</b>	Micrographs of spontaneous neoplasm from the groin of the mice at various magnifications. The histological picture corresponds to epidermal cyst of the skin with signs of suppuration of the wall.....	13
<b>Figure S17.</b>	Chemical structure of $[^{68}\text{Ga}]$ Ga-FA-I (VII) and $[^{68}\text{Ga}]$ Ga-FA-II (VIII) in comparison with other published folate-based conjugates tested with radiogallium.....	14

8 **NMR**9 *Experiment details*

10  $^1\text{H}$  and  $^{13}\text{C}$  NMR spectra were registered on a Bruker Avance 400 spectrometer (400 MHz for  $^1\text{H}$  and  
 11 90 MHz for  $^{13}\text{C}$ ) in  $\text{CDCl}_3$  or  $\text{DMSO-d}_6$ .

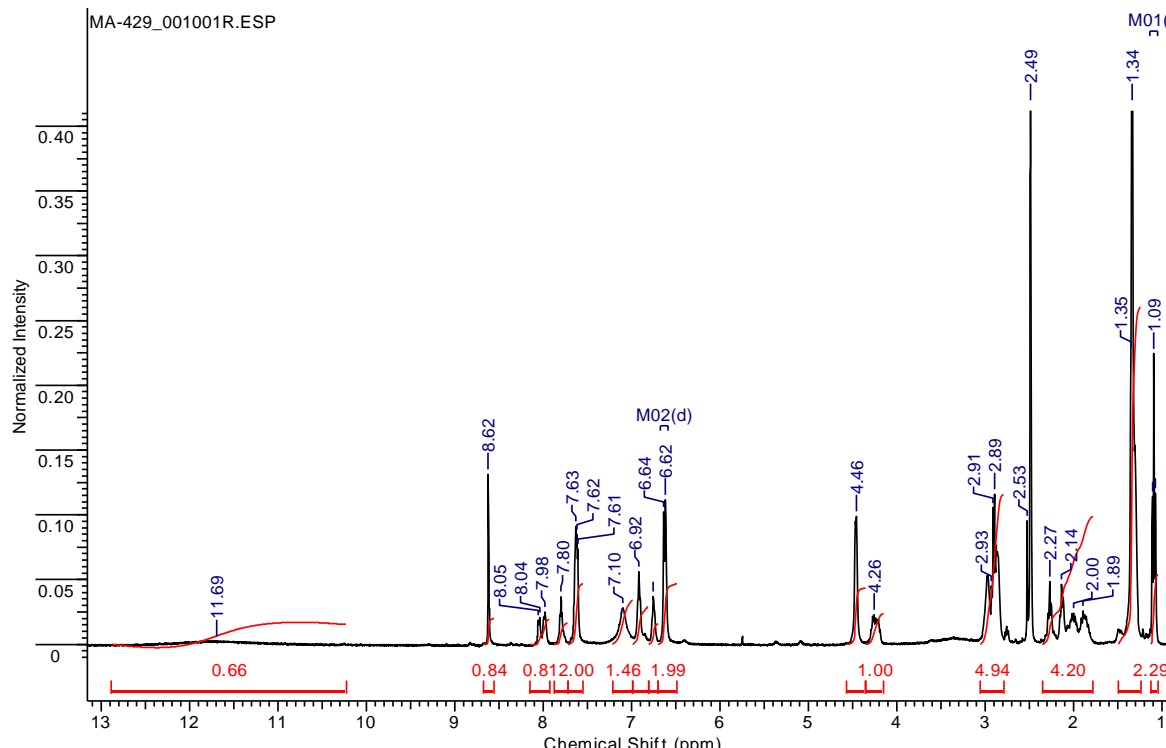


Figure S1.  $^1\text{H}$  NMR spectrum (400 MHz) of **1** in  $\text{DMSO-d}_6$

12  
13

14

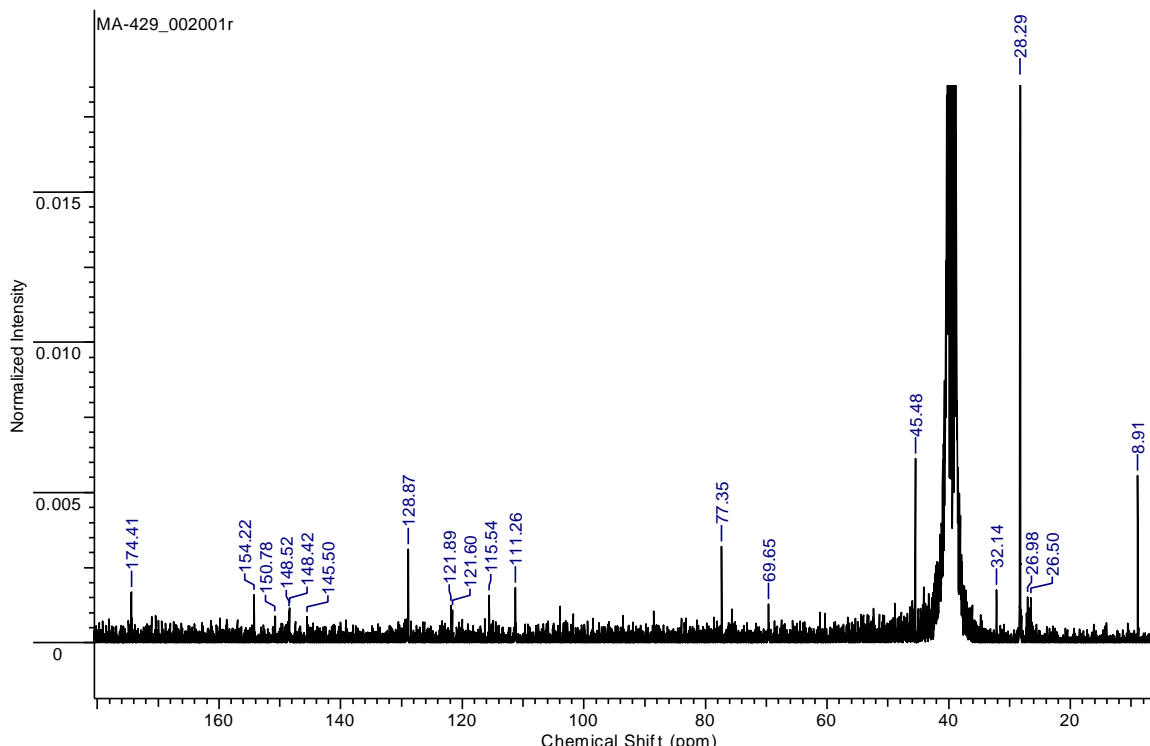
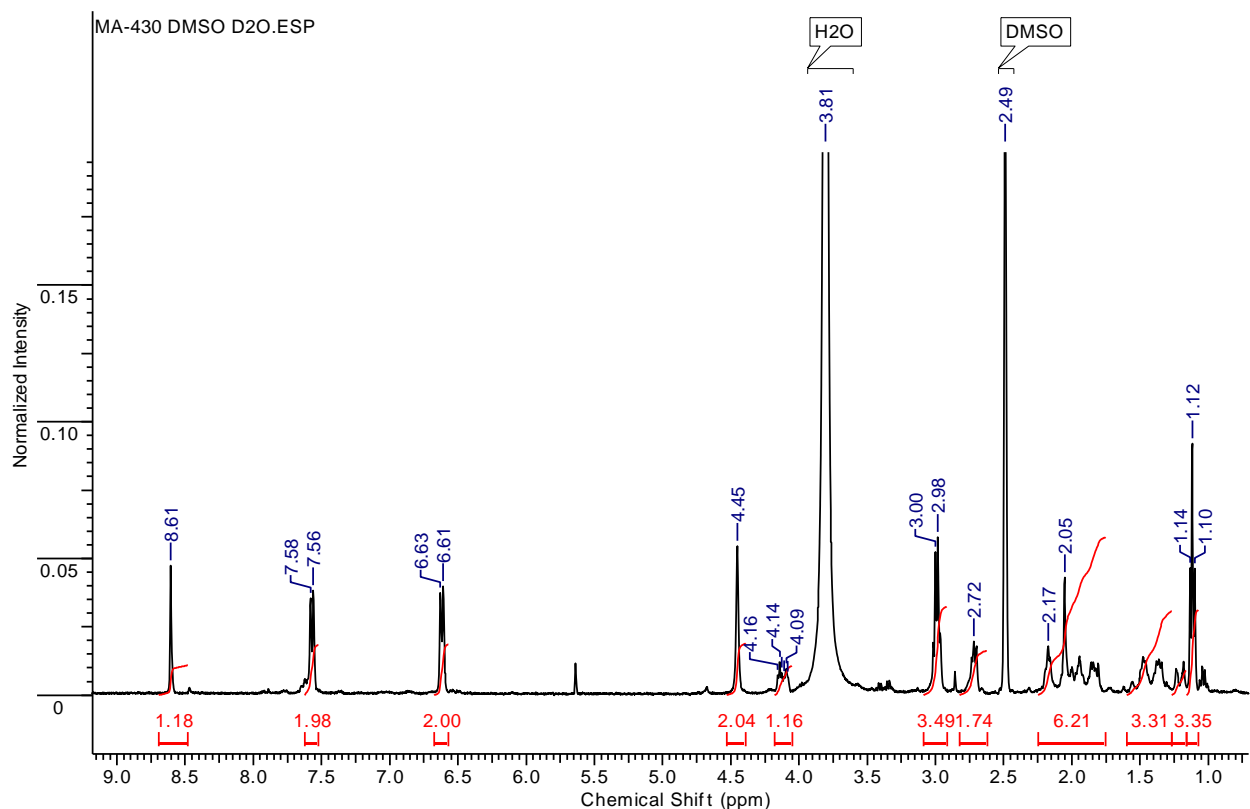


Figure S2.  $^{13}\text{C}$  NMR spectrum (101 MHz) of **1** in  $\text{CDCl}_3$

15  
16



**Figure S3.** <sup>1</sup>H NMR spectrum (400 MHz) of 1 in DMSO-d<sub>6</sub>/D<sub>2</sub>O

17  
18

19

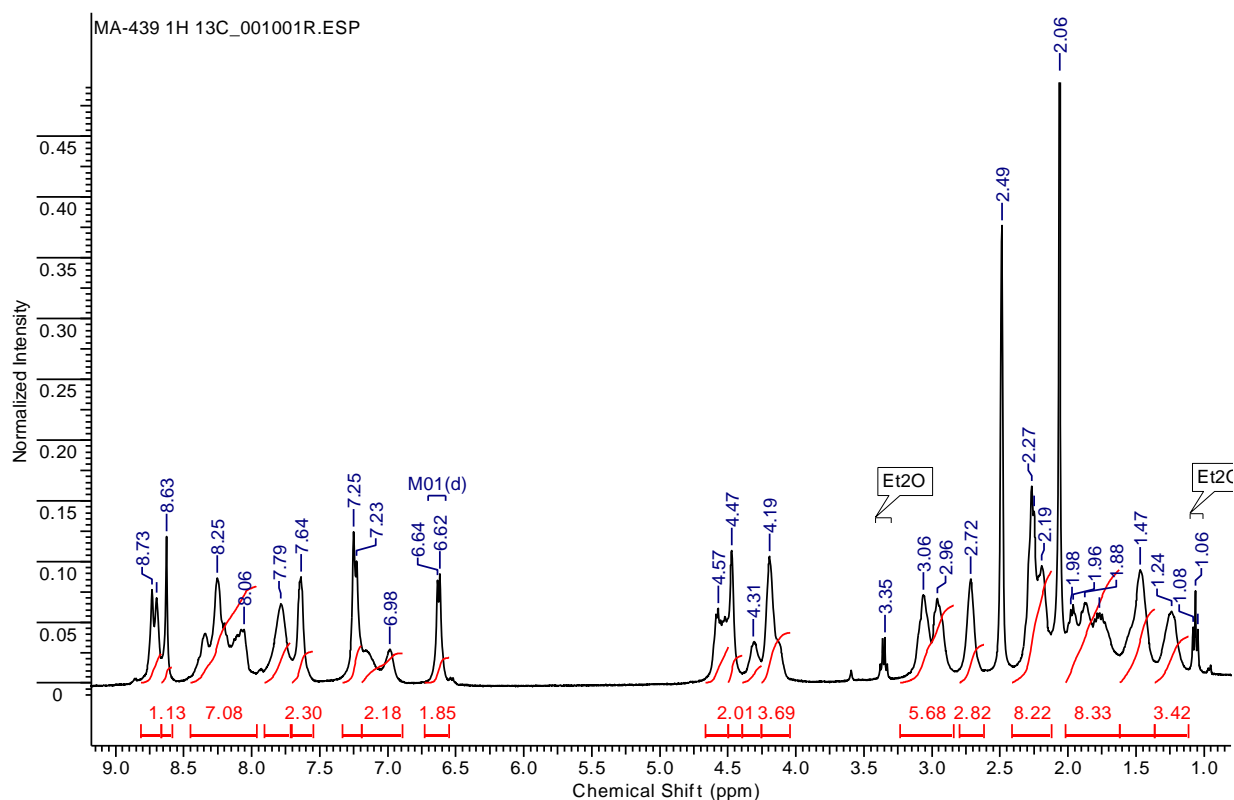
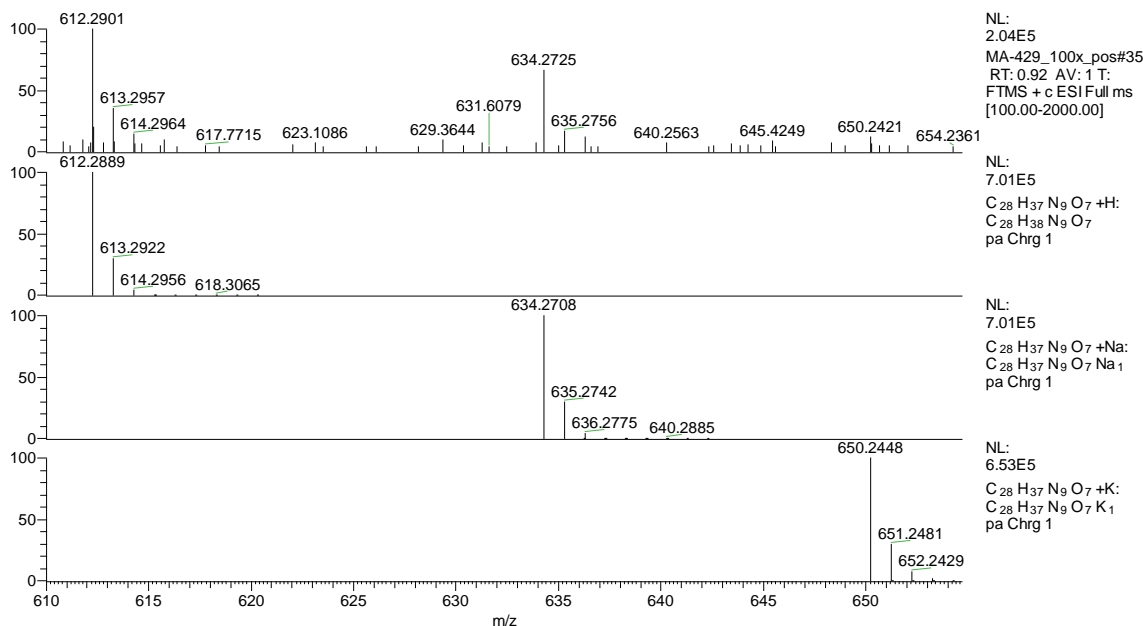


**Figure S4.** <sup>1</sup>H NMR spectrum (400 MHz) of 7 in DMSO-d<sub>6</sub>

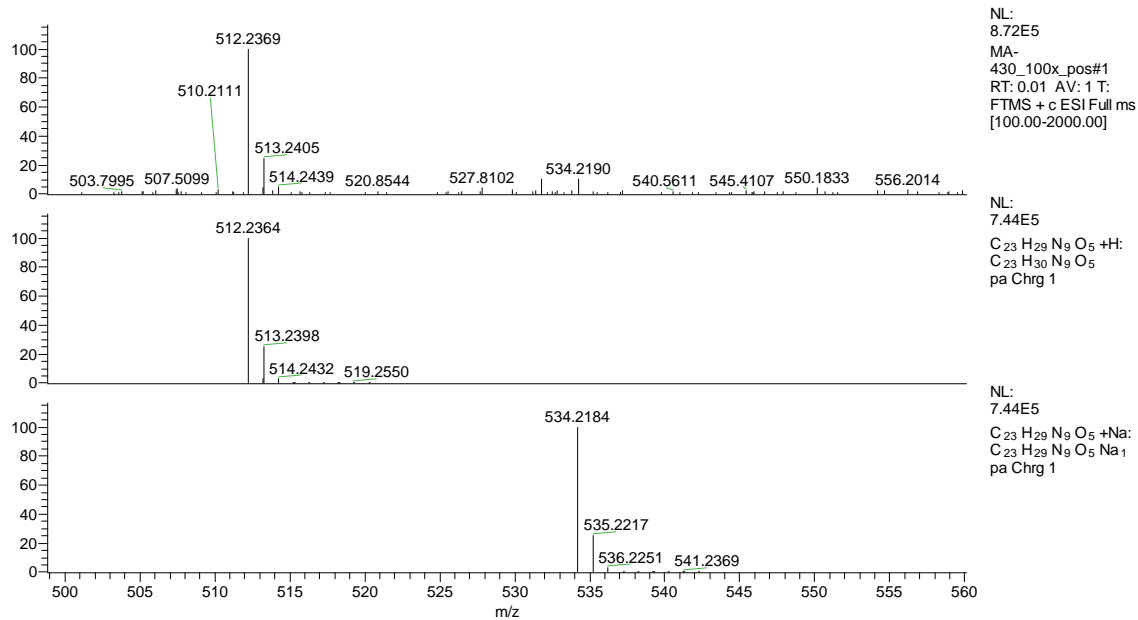
20  
21  
22

23 **HRMS (ESI)**24 *Experiment details*

25 High resolution mass spectra were registered by an Orbitrap Elite mass spectrometer (Thermo  
 26 Scientific) with an ESI ionization source. Compounds with a concentration of 0.1–9 µg/mL (in 1%  
 27 formic acid in acetonitrile) were directly infused into the ion source with a syringe pump (5 µl/min).  
 28 We did not use auxiliary and sheath gases, the spray voltage was +3.5 kV, and the capillary  
 29 temperature was 275°C. The MS spectra were registered by an Orbitrap analyzer with 480000  
 30 resolution (1 microscan, AGC target value of 1e6, max inject time 900 ms, averaged on 9 spectra, MS  
 31 range 90–2000 Da, in some cases 200–4000 Da). We used DMSO and di-iso-octyl phthalate as  
 32 internal calibration signals ( $m/z$  157.03515 and 413.26623) in positive mode and dodecylsulfate ( $m/z$   
 33 265.14790) in negative mode.



34  
35

**Figure S5.** HRMS (ESI) spectrum of **1**

36  
37

**Figure S6.** HRMS (ESI) spectrum of **2**

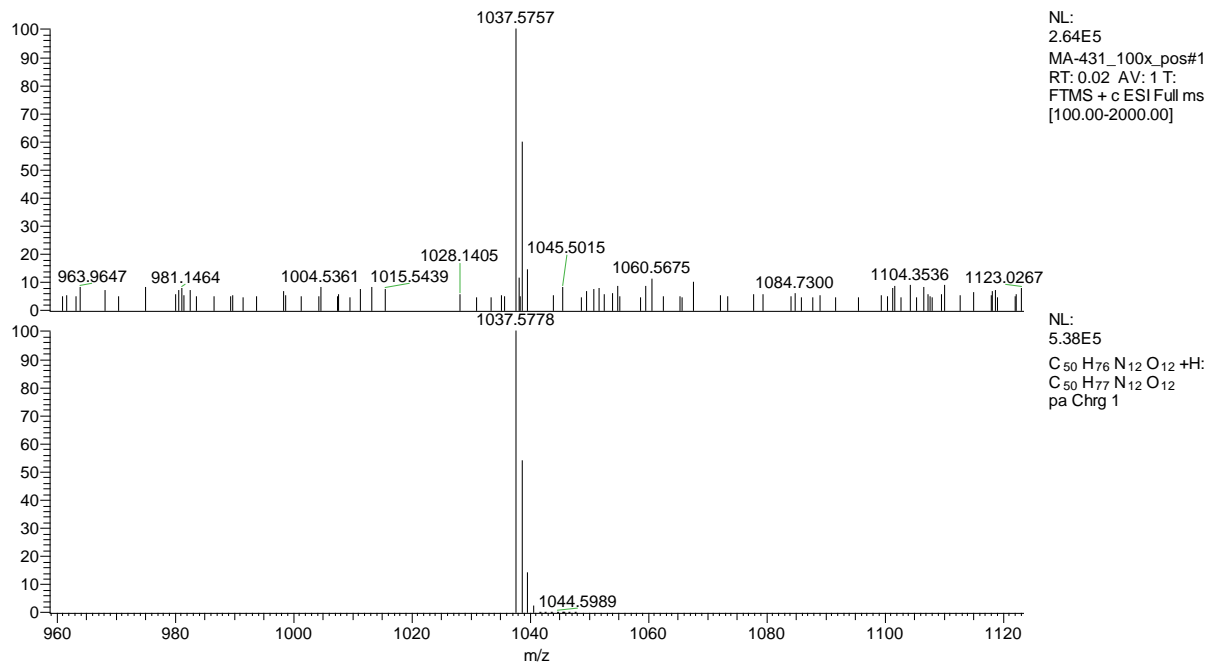
38  
39

Figure S7. HRMS (ESI) spectrum of 3

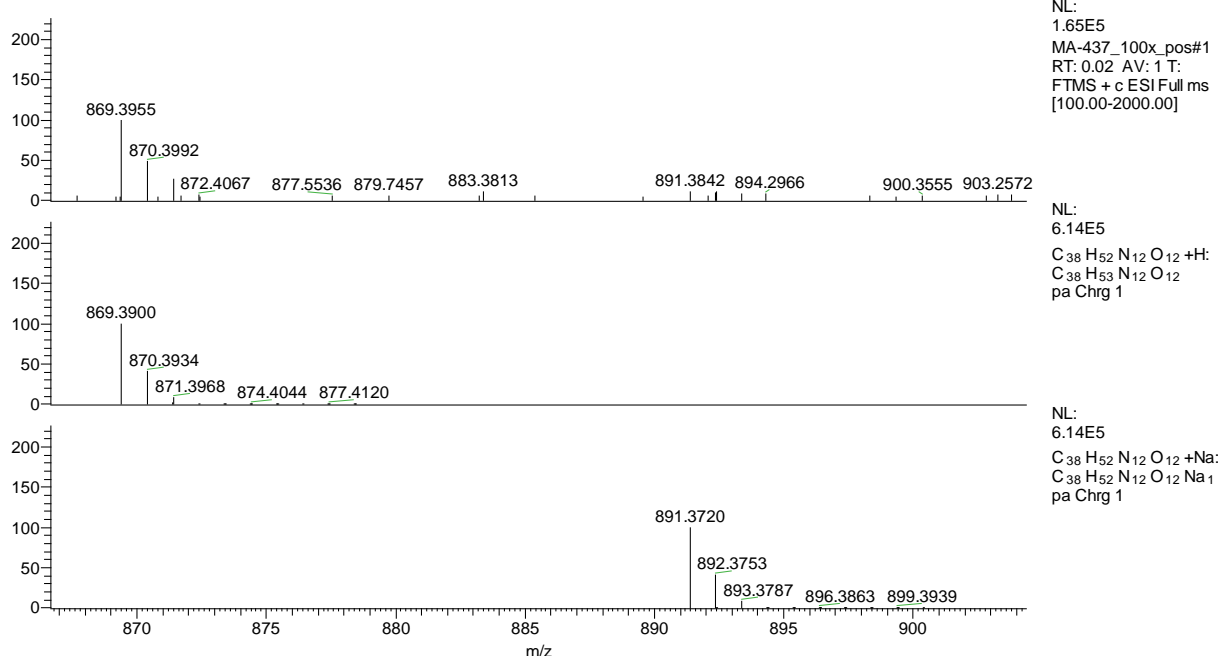
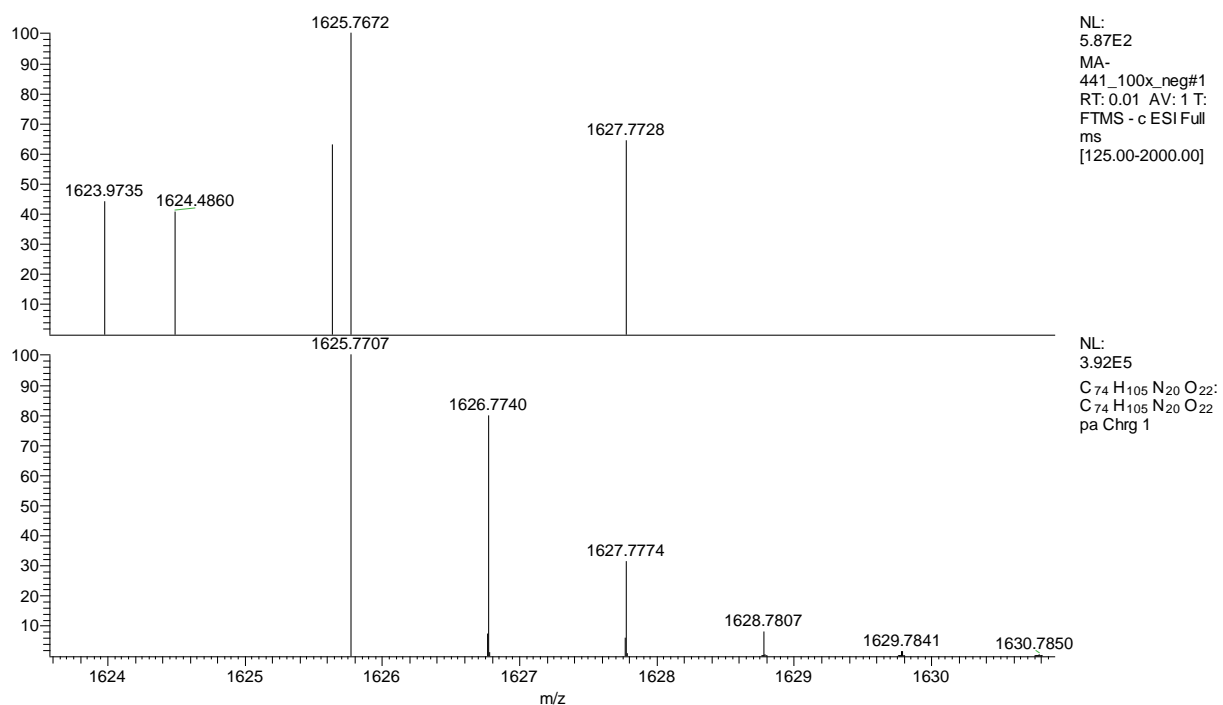
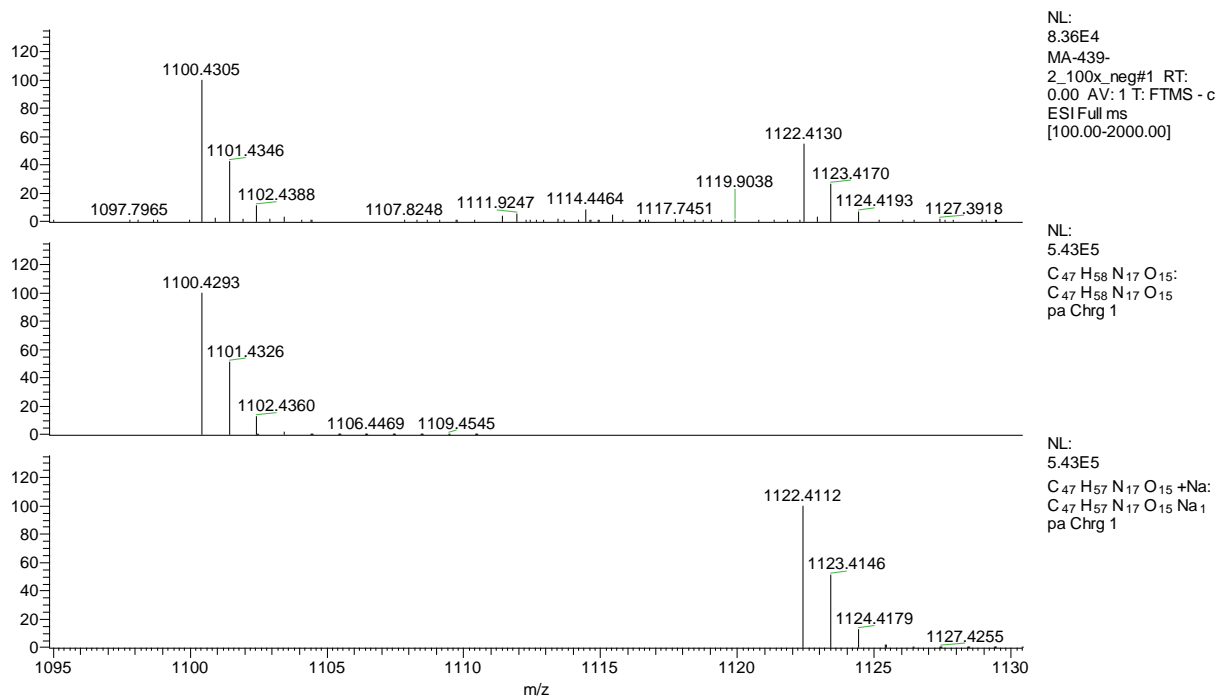
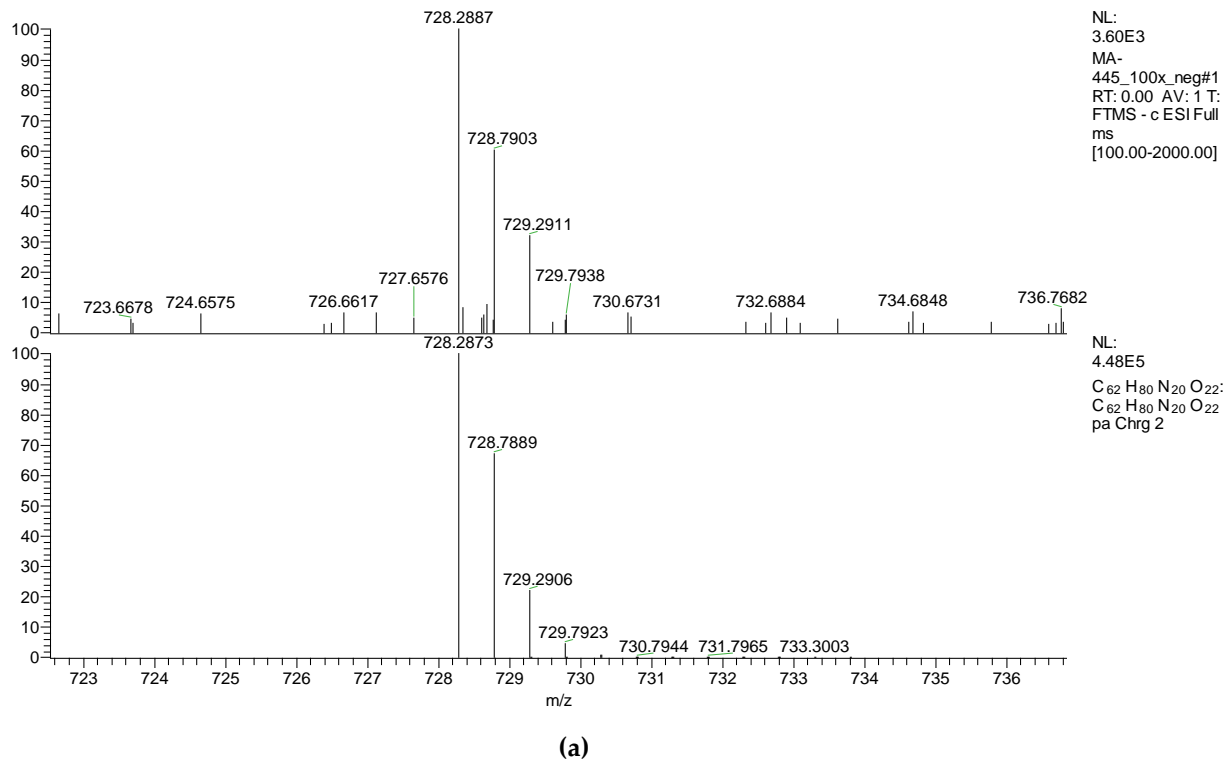
40  
41  
42

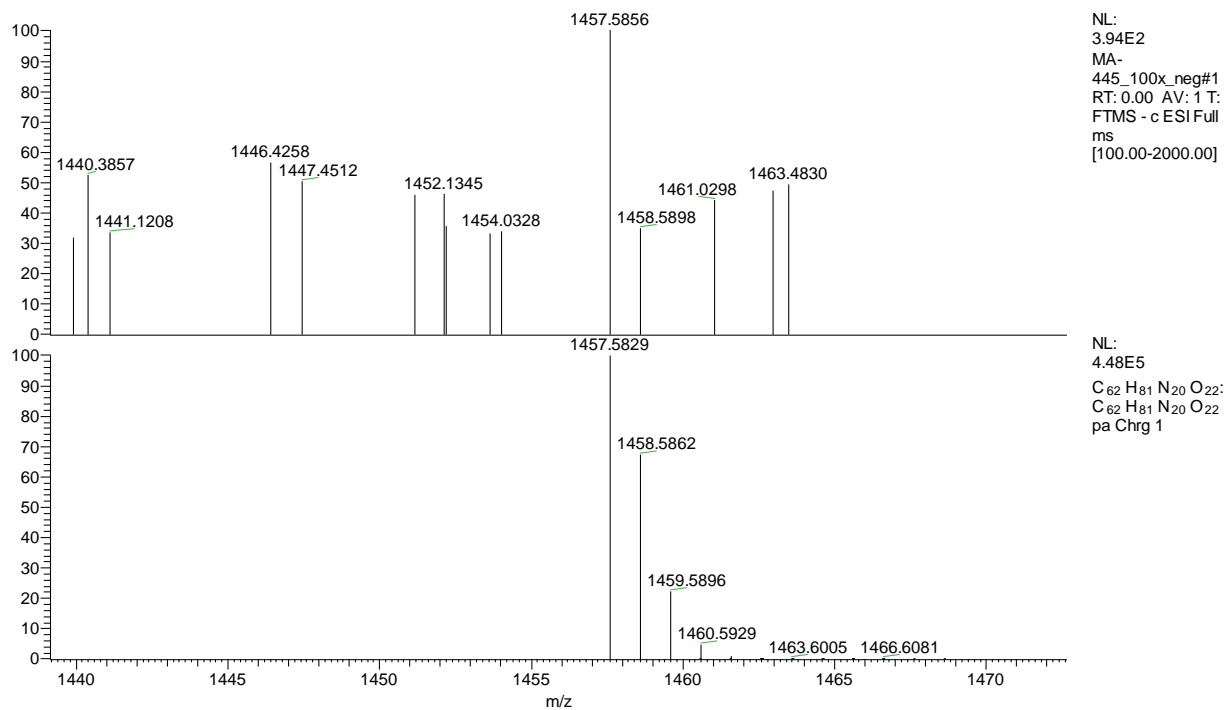
Figure S8. HRMS (ESI) spectrum of 4





48  
49

(a)



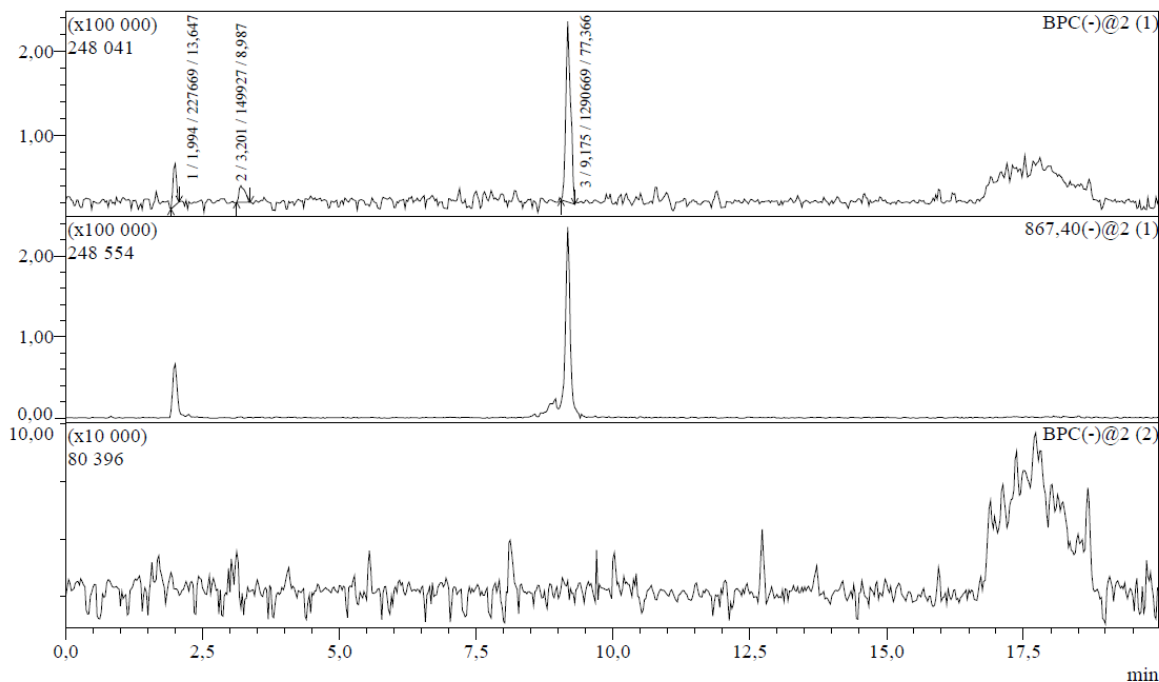
50  
51  
52  
53

(b)

**Figure S11.** HRMS (ESI) spectra of **9**: double charged ion -  $[M-2H]^{2-}$  (a), single charged ion  $[M-H]^-$  (b)

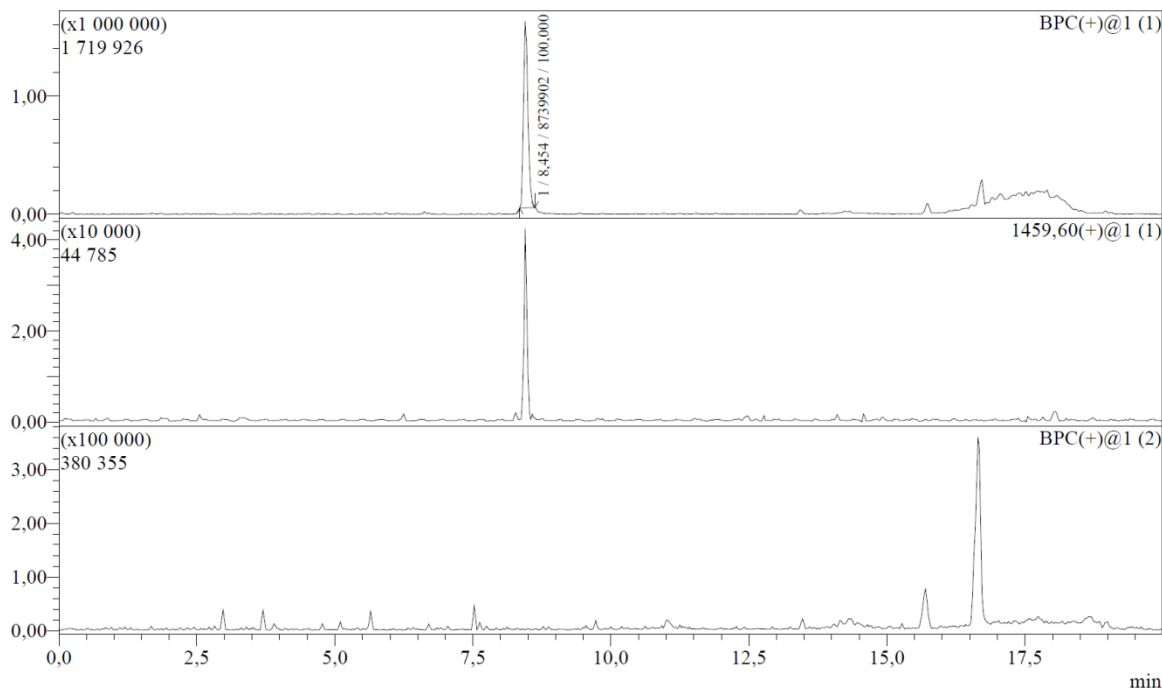
54 **HPLC-MS**55 *Experiment details*

56 For analysis of samples Shimadzu Prominence LC-20 system was used with Phenomenex Luna C18  
 57 column (3 µm, 90 Å, 150 x 4.6 mm) in a column oven at 40°C and a fraction collector coupled to  
 58 single quadrupole mass spectrometer Shimadzu LCMS-2020 with a dual DUIS-ESI-APCI ionization  
 59 source. The mobile phases were A – 0.1% formic acid in water, D – acetonitrile. The LC parameters  
 60 for analyses were a gradient flow of 1 mL/min (0–0.5 min with 5% D, 0.5–9.5 min with 5% to 90% D,  
 61 9.5–12 min with 90% D, 12–14.5 min with 90% to 5% D) with optional UV detection. The MS  
 62 parameters were drying gas 15.0 L/min, nebulizing gas 1.5 L/min, DL temperature 250°C, heat block  
 63 temperature 400°C, interface voltage -3.5 kV, and corona needle voltage -3.5 kV. Positive ions (mass  
 64 range 250–2000 Da, in some cases 155–2000 Da) and negative ions (mass range 90–2000 Da) were  
 65 registered simultaneously.

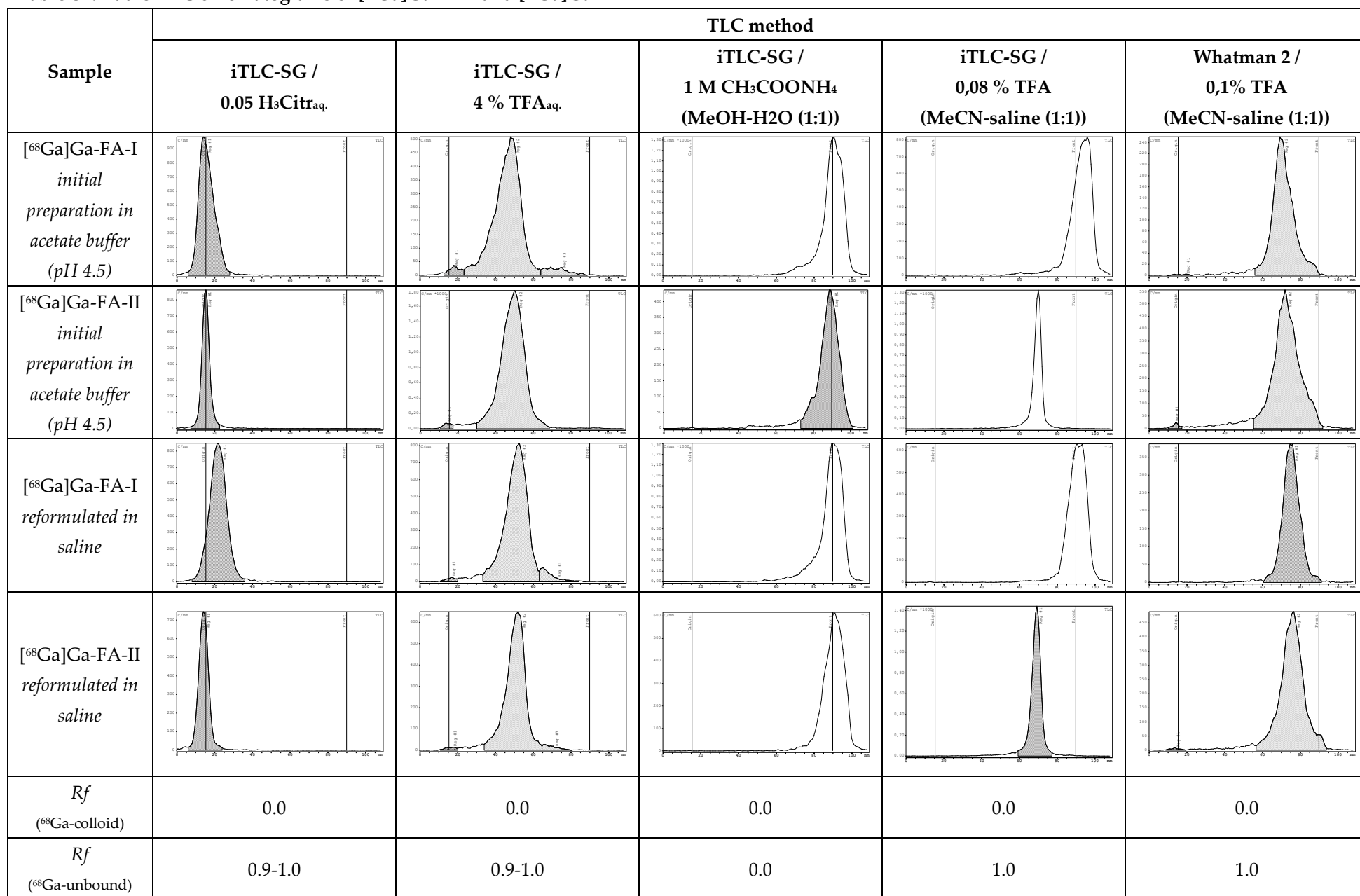


66

67 **Figure S12.** LC-MS chromatogram of **4 (FA-I)**, top - base peak chromatogram of the sample; middle -  
 68 extracted-ion chromatogram of targeted ion; bottom - base peak chromatogram of the blank  
 69 sample).

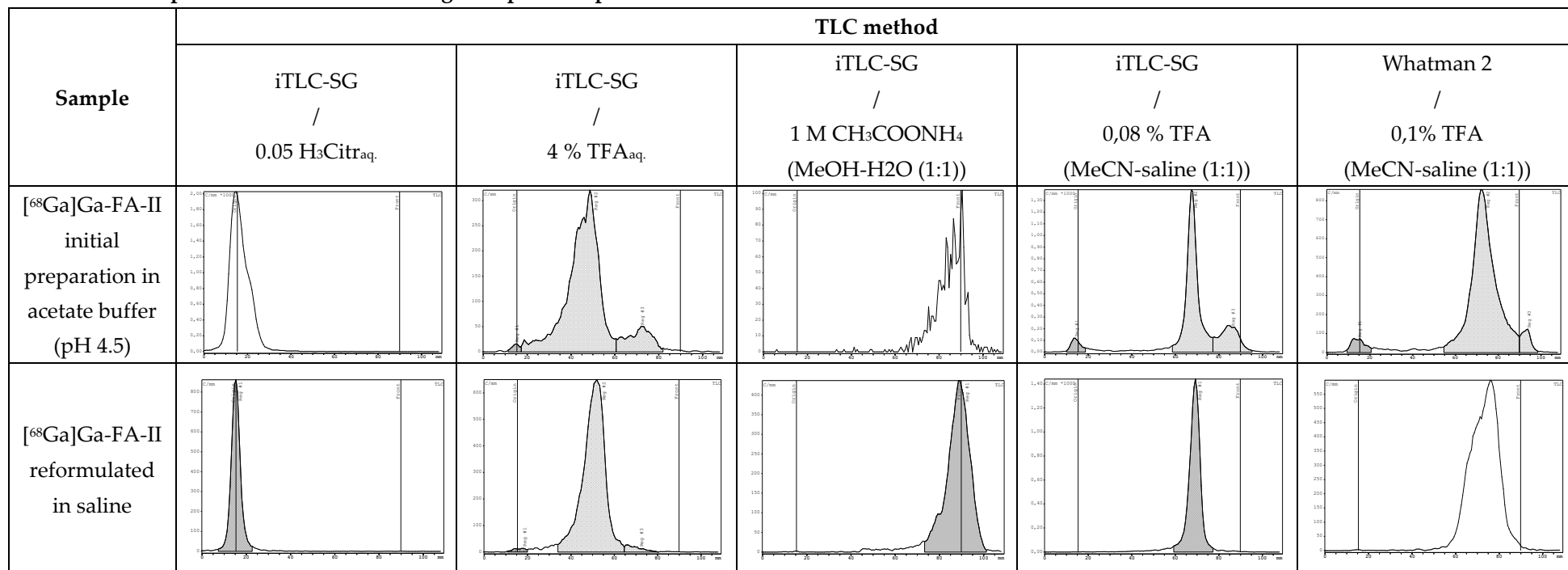


## 75 Radio-TLC

76 Table S1. Radio-TLC chromatograms of [<sup>68</sup>Ga]Ga-FA-I and [<sup>68</sup>Ga]Ga-FA-II

77

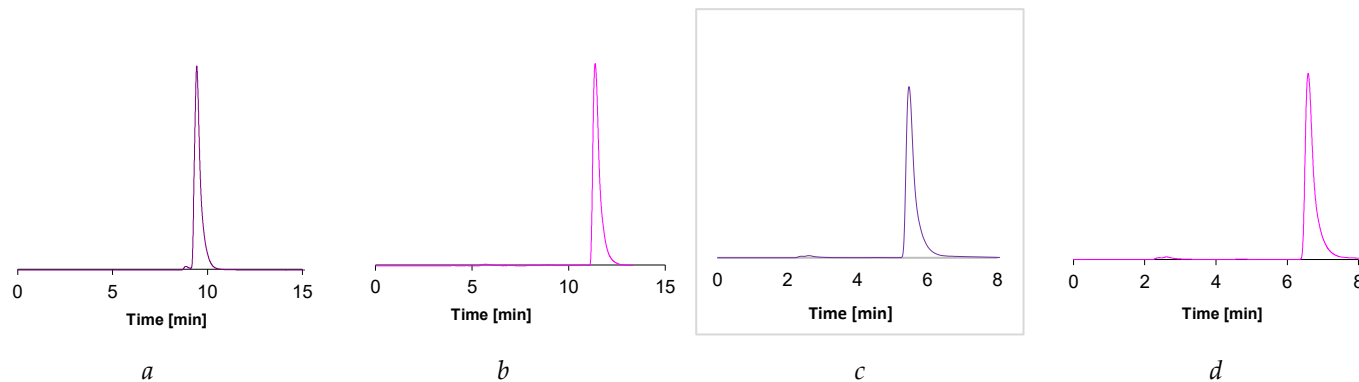
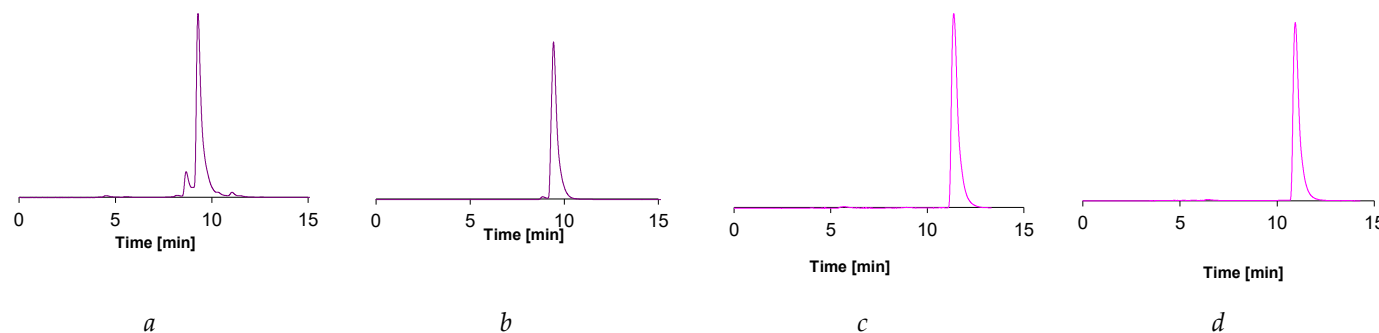
Table S2. Examples of radio-TLC chromatograms pre- and post-reformulation



78

79

## 80 Radio-HPLC

81 **Figure S14.** HPLC chromatograms obtained with Method 1 for  $[^{68}\text{Ga}]\text{Ga-FA-I}$  (*a*) and  $[^{68}\text{Ga}]\text{Ga-FA-II}$  (*b*), and with Method 2 for  $[^{68}\text{Ga}]\text{Ga-FA-I}$  (*c*) and  $[^{68}\text{Ga}]\text{Ga-FA-II}$  (*d*)82 **Figure S15.** HPLC chromatograms obtained with Method 1 for  $[^{68}\text{Ga}]\text{Ga-FA-I}$  pre- (*a*) and post-reformulation (*b*) and for  $[^{68}\text{Ga}]\text{Ga-FA-II}$  pre- (*c*) and post-reformulation (*d*)

83 **The case of [<sup>68</sup>Ga]Ga-FA-I accumulation in non-tumor neoplasm (cyst)**

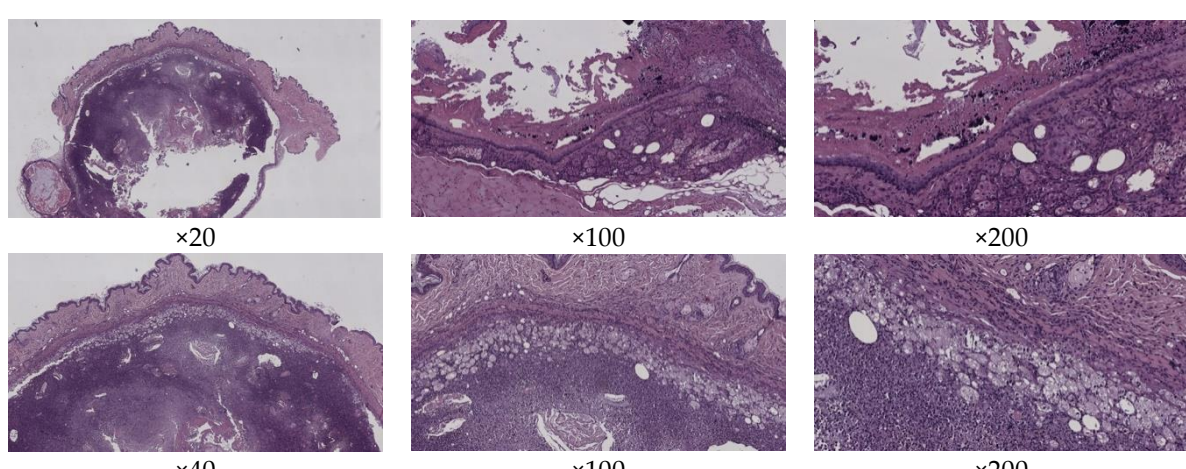
84 During the biodistribution study of [<sup>68</sup>Ga]Ga-FA-I in immunodeficient mice with transplanted KB tumors, one of the  
 85 mice autopsy (at the time point of 30 min) revealed a spontaneous neoplasm in the groin area. This neoplasm was  
 86 included in the layout of organs for measurement by direct radiometry. The measurement results are presented in  
 87 Table S3 (these results were not included in data presented in Tables 3, 4). Histological examination showed that this  
 88 neoplasm is a cyst (Figure S16).

89 A small area of a large cyst surface is lined with stratified squamous epithelium, the lining is absent for the rest of  
 90 it. Inflammatory infiltrates of lymphocytes and neutrophils, as well as assemblies of foamy macrophages, were found  
 91 in the cyst wall. In the lumen of the cyst keratin-filled nodules, foamy macrophages and neutrophils were found.  
 92 Interestingly, in addition to the high content of [<sup>68</sup>Ga]Ga-FA-I in the blood (3.27% versus the average value of  $1.37 \pm$   
 93 0.38%, 30 min after administration), its accumulation in the cyst was higher than that in KB tumor of the same animal  
 94 (2.44% versus 1.75% ID/g).

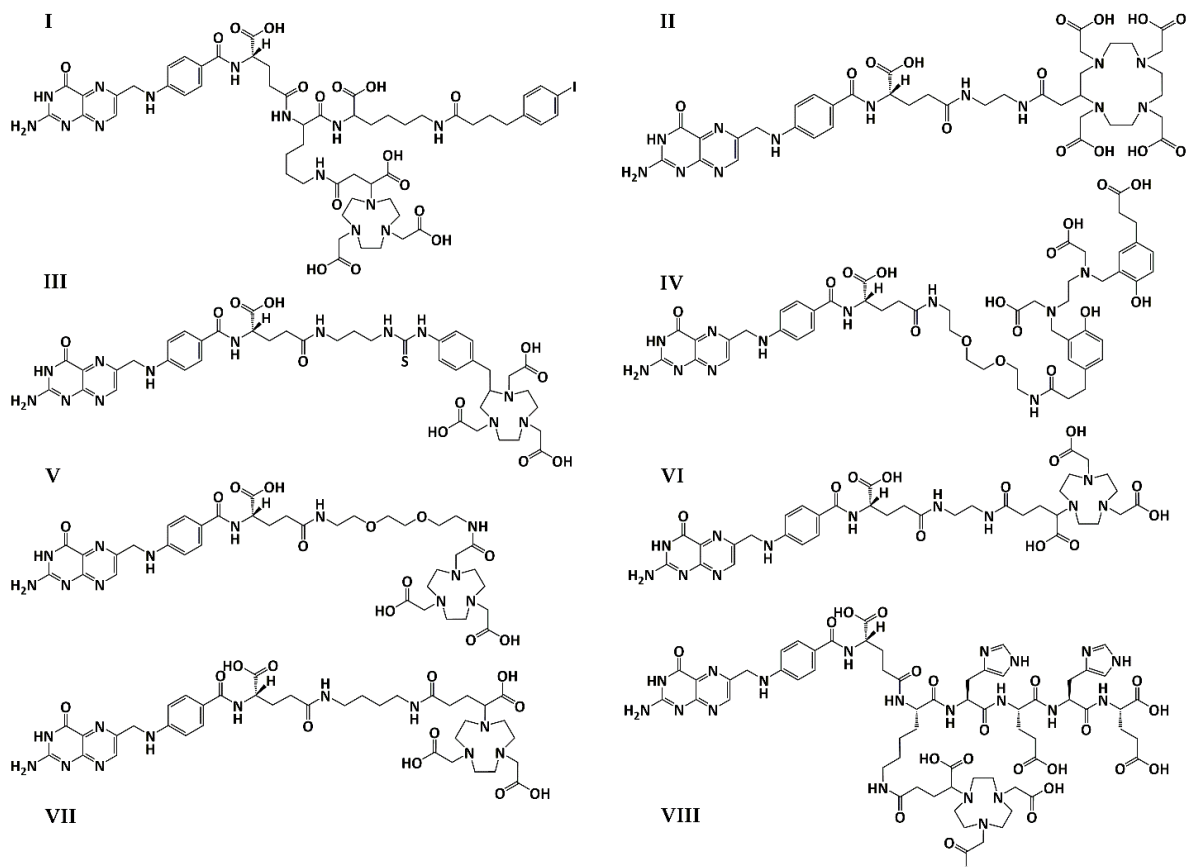
95 Taking into account the data of histological examination, as well as the fact that experiments on the binding of  
 96 [<sup>68</sup>Ga]Ga-FA-I and [<sup>68</sup>Ga]Ga-FA-II to blood leukocytes showed almost zero result (not presented), it can be assumed  
 97 that the activity accumulated in the cyst is associated precisely with activated macrophages (in specific, foam cells),  
 98 which is consistent with published data [8,9]. However, the uptake of the cyst is very similar to that of highly perfused  
 99 organs (liver, lungs), so potentially perfusion itself could be imputable for the higher uptake in the cyst. Further  
 100 research is needed to confirm the nature of this process.

101 **Table S3.** Biodistribution of [<sup>68</sup>Ga]Ga-FA-I in KB-tumor bearing BALB/c nude mouse with spontaneous neoplasm 30 min  
 102 after injection

Tissue/ Organ	ID/g, %
blood	3.27
lungs	2.83
heart	1.51
stomach	0.67
spleen	0.89
liver	2.48
kidneys	14.68
bladder	1.19
intestines	1.07
brain	0.18
muscle	0.37
tumor (KB)	1.75
neoplasm (cyst)	2.44



103 **Figure S16.** Micrographs of spontaneous neoplasm from the groin of the mice at various magnifications. The histological picture  
 104 corresponds to epidermal cyst of the skin with signs of suppuration of the wall.



107  
108 **Figure S17.** Chemical structure of  $[^{68}\text{Ga}]\text{Ga-FA-I}$  (**VII**) and  $[^{68}\text{Ga}]\text{Ga-FA-II}$  (**VIII**) in comparison with other published  
109 folate-based conjugates tested with radiogallium (for references see **Tables 5, 6**).

110